GENERALIZED MULTI-IMPULSIVE MANEUVERS FOR OPTIMUM SPACECRAFT RENDEZVOUS

G. Gaias[1], S. D'Amico[2], and J.-S. Ardaens[3]
[1][2][3] *German Aerospace Center (DLR), Münchner Str. 20, 82234 Wessling, Germany,*
0049 8153 28-1769, gabriella.gaias@dlr.de,
0049 8153 28-2115, simone.damico@dlr.de,
0049 8153 28-2141, jean-sebastien.ardaens@dlr.de.

Abstract: *This work describes the design of an impulsive maneuvers' planner meant for on-board autonomous optimum formation flying reconfigurations. The whole variation of the relative orbit is stepwise achieved through intermediate configurations, so that passive safety and delta-v consumption minimization are pursued. The description of the relative motion is accomplished in terms of relative orbital elements and the reconfiguration plan takes into account mean effects due to the Earth oblateness coefficient and differential drag. Maneuvers consist of sets of triple tangential impulses and a single out-of-plane burn to establish each intermediate configuration. They are scheduled in time intervals compliant with the user-defined permissible time control windows.*

Keywords: *Formation reconfiguration, Autonomy, Relative orbital elements.*

1. Introduction

Spacecraft formation-flying and on-orbit servicing missions require the capability to establish and reconfigure the relative motion of co-orbiting vehicles in a safe, accurate and fuel-efficient manner. Typical operational scenarios of such distributed space systems prescribe maneuvering time constraints dictated by the satellite bus and payload needs, by available ground support and ground contact issues. This work addresses the design and development of a flexible maneuver planning framework for autonomous optimum formation reconfiguration over a given time interval including user-defined permissible control windows.

Various control methods for spacecraft rendezvous have been presented in literature - continuous and discrete, numerical and analytical, for circular and eccentric orbits, using relative Cartesian coordinates and orbital elements. Whereas the most recent flight demonstrations of autonomous formation control are represented by the experiments on the PRISMA mission [1], among them the Spaceborne Autonomous Formation Flying Experiment (SAFE) [2] and by the TanDEM-X Autonomous Formation Flying (TAFF) system [3]. These systems rely on practical and simple closed-form solutions of the Gauss' variational equations which can be expressed analytically and be efficiently embedded into spaceborne microprocessors.
TAFF makes use of pairs of (anti-)along-track maneuvers separated by half an orbital revolution for in-plane formation keeping only, whereas SAFE is able to exploit radial and cross-track pulses for enhanced in-plane and out-of-plane control respectively. The logic which triggers the execution of maneuvers is based either on a fixed maneuver cycle (TAFF) or on the violation of predefined control windows defined about nominal relative orbital elements (SAFE). Although the necessary maneuvers are autonomously planned and executed on-board based on the most recent estimates of the relative orbital elements, the nominal or desired formation

configurations (i.e., guidance) are still prescribed from ground through telecommands and thus with man-in-the-loop.
This work builds on the state-of-the-art in an attempt to generalize the SAFE and TAFF algorithms in order to improve the autonomy (including guidance) and flexibility (including constraints) of flight-proven methodologies without sacrificing simplicity and determinism to the largest possible extent. Although the focus is on formations with an active chief satellite in near-circular orbit about an oblate Earth, the approach is kept as general as possible to allow for future extension to eccentric perturbed orbits. In contrast to previous flight systems which rely on GPS relative navigation, here observability issues related to angles-only navigation are taken into account to support far-range non-cooperative rendezvous scenarios as well. The main goal is to compute the guidance profile on-board as a sequence of intermediate desired formation configurations pursuing certain optimality criteria. This translates into an optimization problem where an aimed final formation has to be acquired in a defined time period while maximizing the satisfaction of the prescribed criteria. Operationally the minimization of the total delta-v consumption and the maximization of the navigation system observability are sought.

The paper is organized as follows. First of all the overall concept of the planner is described. Second it is explained what solutions are employed respectively for the guidance and control problems. The objective of this first topic is to provide a set of intermediate relative orbits to be acquired at certain intermediate times (related to the schedule of the allowed maneuver windows) in order to achieve the final aimed relative state. The local control task, instead, deals with the problem of establishing any intermediate relative geometry in a limited and fixed time period. Finally an example showing the functioning of the planner is provided and discussed.

2. Overall Concept

The objective of the generalized multi-impulsive maneuvers controller is to provide the sequence of maneuvers needed starting from an initial time to achieve a prescribed relative orbit at a given final time. Thus the controller prototyped in this research delivers an open-loop maneuver profile that covers the whole reconfiguration's horizon.

In agreement and continuation of previous work conducted by the authors, relative orbital elements (ROE) are used to parameterize the relative dynamics. They consist of a set of six elements with an immediate geometrical meaning of the characteristics of the relative orbit that they represent. They are defined as:

$$\delta\boldsymbol{\alpha} = \begin{pmatrix} \delta a \\ \delta\lambda \\ \delta e_x \\ \delta e_y \\ \delta i_x \\ \delta i_y \end{pmatrix} = \begin{pmatrix} \delta a \\ \delta\lambda \\ \delta e\cos\varphi \\ \delta e\sin\varphi \\ \delta i\cos\theta \\ \delta i\sin\theta \end{pmatrix} = \begin{pmatrix} (a-a_\mathsf{d})/a_\mathsf{d} \\ u-u_\mathsf{d}+(\Omega-\Omega_\mathsf{d})\cos i_\mathsf{d} \\ e\cos\omega - e_\mathsf{d}\cos\omega_\mathsf{d} \\ e\sin\omega - e_\mathsf{d}\sin\omega_\mathsf{d} \\ i-i_\mathsf{d} \\ (\Omega-\Omega_\mathsf{d})\sin i_\mathsf{d} \end{pmatrix} \tag{1}$$

where a, e, i, ω, Ω, and M denote the classical Keplerian elements, and $u = M + \omega$ is the mean argument of latitude. The subscript "d" labels the deputy spacecraft of the formation,

which, in this work, plays the role of the maneuverable servicer satellite. In the sequel all absolute quantities refer to the servicer satellite, thus the subscript is dropped. The quantities $\delta\mathbf{e} = (\delta e \cos\varphi \;\; \delta e \sin\varphi)^{\mathsf{T}}$ and $\delta\mathbf{i} = (\delta i \cos\theta \;\; \delta i \sin\theta)^{\mathsf{T}}$ define the relative eccentricity and inclination vectors. Under the assumptions of the Hill-Clohessy-Wilshire equations (HCW) their magnitudes δe and δi express the in-plane and out-of-plane amplitudes of the oscillations of the relative motion respectively. The phase angles φ and θ identify the relative perigee and relative ascending node of the relative orbit. Therefore $\delta\mathbf{e}$ and $\delta\mathbf{i}$ fully describe the orientation and the shape of the relative motion. The remaining ROE, the relative semi-major axis δa and the relative mean longitude $\delta\lambda$ provide the mean offsets in local radial and local along-track directions of the orbital frame respectively. When both the satellites belong to Keplerian orbits, only the element $\delta\lambda$ varies with time according to:

$$\delta\lambda(t) = -1.5n(t - t_0)\delta a_0 + \delta\lambda_0 \tag{2}$$

thus δa embodies the drift coefficient of the relative motion. The detailed description of the ROE, together with the development and discussion of the model of the relative dynamics and its extension to include differential drag and secular effects due to the J_2 perturbation is given in [4]. This topic is further addressed in section 3.

By letting $\mathbf{P}$ identifying the dimensional point in the ROE space (i.e. $\mathbf{P}(t) = a\delta\boldsymbol{\alpha}(t)$), a reconfiguration from a certain initial relative orbit to an aimed final one can be defined as the transition $\mathbf{P}_0 \rightarrow \mathbf{P}_{\mathsf{F}}$ over the finite time interval $[t_0, t_{\mathsf{F}}]$. The main concept of the controller consists in splitting the reconfiguration problem into two layers:

1. *guidance*, that is the computation of some (optimal with respect to a given criterion) intermediate configurations $\mathbf{P}_{\mathsf{i}}$ to be reached at the given times t_i, in order to achieve the final aimed $\mathbf{P}_{\mathsf{F}}$.

2. *control*, that is the local resolution of the *i*-th problem of establishing any intermediate $\mathbf{P}_{\mathsf{i}}$ in a limited (and specified) time horizon that ends at t_i.

The idea that motivates such a layered approach is to simplify the problem by decoupling the geometry of the relative orbits from the computation of the maneuvers to establish such motions. Thus, as seen by the guidance layer, the ROE evolve according to the model of the dynamics until some discontinuities occur. These represent the global effect of the bunch of maneuvers that would be needed to accomplish such jumps of ROE. It is emphasized that, this approach allows immediately recognizing un-safe or un-feasible configurations, since they correspond to $\mathbf{P}_i$ points in forbidden regions of the state space. Whenever the merit criterion of the planning problem can be written as function of the variations of ROE, then the guidance output comes from the solution of an optimum problem where the variations of ROE that have to occur over each allowed maneuver window are taken as control variables.
On the other hand, the local problem focuses on the computation of the locations and the magnitudes of the maneuvers that allow achieving an aimed variation of ROE. Within the assumptions of Keplerian motion, the out-of-plane and in-plane motions are decoupled. The out-of-plane reconfiguration reduces to the deterministic problem of computing the cross-track thrust and its burn time to realize a given change in the relative inclination vector.

The in-plane reconfiguration problem, instead, requires at least two burns in order to realize any given change in the four in-plane ROE. This translates into an underdetermined system with six unknowns (i.e. time, radial and tangential delta-v magnitudes for each maneuver) in four equations. It can be shown that two-impulses reconfiguration schemes require a numerical solution method in order to realize any given set of in-plane ROE variation. Fully analytical solution schemes exist when three impulses are used instead. Specifically these employ pure tangential maneuvers that occur at half orbital period multiples of the mean argument of latitude equal to the phase angle of the total aimed variation of the relative eccentricity vector. This topic is further tackled in section 4.

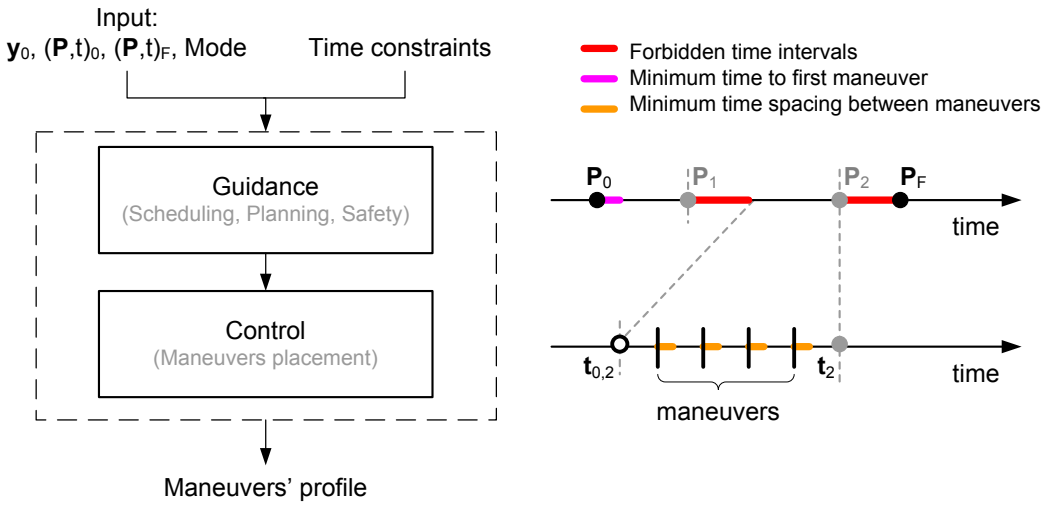

Figure 1. Structure of the maneuver planner

Figure 1 provides a schematic description of the layered structure of the planner: the main tasks of each layer are specified. Concerning the interfaces to the controller, inputs consist of the absolute state of the servicer $\mathbf{y_0}$, the so far estimated set of ROE $\mathbf{P}_0$(both at the initial time t_0), the aimed final orbit $\mathbf{P}_F$, and the final time t_F. Time constraints of an operative scenario are represented by: time intervals in which it is not allowed maneuvering, the minimum time from the generation of the maneuvers profile to the first command, and the minimum time spacing between different maneuvers to let the spacecraft being prepared with proper attitude and thrusters' state. Other typical constraints are the minimum delta-v impulse, the maximum allowed magnitude of a delta-v, minimum separations respectively perpendicular and aligned to the flight direction, and, in case of vision-based rendezvous, target visibility constraints [5]. Depending on the desired operative mode (see section 2.1), the maneuver planner foresees a reconfiguration in only one step (*minimum delta-v* mode) or plans intermediate configurations delimited by the forbidden time intervals defined by the user (*maximum observability* mode).

2.1. Operative Modes

The lower bound of the delta-v expenditure to accomplish an in-plane formation reconfiguration is known [6-7]: it requires to exploit only tangential burns. By using three impulses an analytical solution exists for any set of aimed correction of in-plane ROE. Moreover, in the typical scenario of a rendezvous, this solution is able to achieve the absolute minimum of the delta-v

cost. With rendezvous scenario it is meant to shrink the relative motion while approaching the target, aiming to a bounded final motion. This is the case in which the change in the shape of the formation ($\Delta\delta\mathbf{e}$) is dominant with respect to the change in the drift ($\Delta\delta a$) since large relative mean longitude transfers occur over long time horizons. The actual computation of the maneuvers is presented later in section 4. Regarding the guidance layer, instead, if the planning criterion is to seek for the minimum delta-v, then no intermediate P_i should be introduced and maneuvers should be placed in agreement with the scheme of section 4. This objective is referred as *minimum delta-v* operative mode.

Although this mode guarantees to spend the minimum delta-v consumption, from an operative point of view this approach presents some not practical aspects. First of all when a servicer satellite approaches a non-cooperative target the errors in the estimated initial relative state P_0 are large [5]. Thus it is typically necessary to update the maneuvers' profile as soon as the knowledge of the relative state is refined. Consequently it is not convenient to perform large (due to the limited number of impulses) maneuvers at the beginning of the rendezvous. Secondly taking into account the effects of the maneuver execution errors, it is not efficient to accomplish a reconfiguration thorough few large maneuvers. On the other hand, if the relative navigation is performed via angles-only measurements the most fruitful way to improve the observability properties of the system is to perform some maneuvers; the more intense the maneuver activity the more observable the relative navigation problem [8]. To this end, it is not convenient to spread the few available impulses over wide time horizons. In an attempt to overcome these practical issues while still pursuing to minimize the fuel consumption during the rendezvous, a *maximum observability* operative mode is designed.
According to it, the rendezvous is accomplished in a step-wise manner through a user-defined number of intermediate configurations to be reached at certain times t_i that are the end time of the windows in which it is allowed maneuvering (see $[t_{0,i}, t_i]$ in Fig. 1). The ROE sets at such intermediate times are computed so that the total delta-v is minimized (see section 3). Clearly having introduced intermediate $\mathbf{P}_i$ the *maximum observability* mode consumes more delta-v than the minimum delta-v one. Nevertheless the user can now intensify the occurrence of maneuvers when convenient due to practical motivations. Therefore the input that lists the forbidden time intervals can also be used to allow a sort of control action of the user over the maneuvers' profile. According to the structure of the controller, both the operative modes make use of the same local control functionality. Consequently, if the forbidden time intervals input is left empty, the observability mode coincides with the minimum delta-v one. Still in this first case no a-posteriori check on the feasibility of the maneuvers' location has to be performed, as all the reconfiguration time horizon is free from forbidden regions (see section 7). A further synergy between the two operative modes is provided by the typology of maneuvers employed. In [8] in fact it was shown that once fixed the magnitude of a maneuver, tangential burns are to be preferred with respect to the radial ones in terms of effects on the observability of the relative navigation problem. This is due to the fact that the drift translates into a more distinguishable pattern of one of the two measured angles with respect to the trend before the maneuver.
Finally, the introduction of intermediate configurations has the positive benefit to strengthen the supervision over safety during the approach. To this aim it is simply needed to verify, and eventually to correct, that the $\mathbf{P}_i$ output by the planner have an adequate relative eccentricity and inclination vectors separation [9].

3. The Planning Problem

This section deals with the solution of the problem of finding m intermediate relative orbits $\mathbf{P}_i$ to be reached at the times t_i in order to perform the reconfiguration $\mathbf{P}_0 \rightarrow \mathbf{P}_\mathsf{F}$ while using the minimum possible delta-v. According to the employed solution method all the intermediate times will be exploited.
The delta-v cost of the plan can be expressed by the following convex form:

$$J_{\text{plan}} = \sum_{i=1}^{m}(\Delta\|\delta\mathbf{i}\|)_i^2 + \sum_{i=1}^{m}(\Delta\delta a)_i^2 + \sum_{i=1}^{m}(\Delta\delta\lambda)_i^2 + \sum_{i=1}^{m}(\Delta\|\delta\mathbf{e}\|)_i^2 \tag{3}$$

where the *i*-th variations of ROE $(\Delta\delta\boldsymbol{\alpha})_i$ that occur at t_i are assumed as control variables. Within the hypothesis of linearized relative motion, the closed form solution of the mean relative motion in the presence of J_2 Earth oblateness effects is presented in Ref. [4, p.34]. The interaction between the satellites and the upper layers of the atmosphere is modeled through a differential drag, which produces an off-set in the along-track direction proportional to the square of the elapsed time, when assuming the atmospheric density constant within few kilometers. Taking into account the property of the relative dynamics expressed by Eq. 2, the effect of the differential drag is introduced in the linear model of the relative dynamics as a linear variation of the relative semi-major axis with respect to the elapsed time [4, p.37]:

$$\delta\dot{a} = -\frac{1}{n}\Delta B\rho v^2 \tag{4}$$

where ΔB is the difference of the ballistic coefficients of the satellites and ρ and v are respectively the atmospheric density and the deputy velocity with respect to the atmosphere. The correspondent complete state transition matrix can be written augmenting the ROE state of Eq.1 with $\delta\dot{a}$:

$$\boldsymbol{\Phi}(\Delta t) = \begin{bmatrix} 1 & 0 & 0 & 0 & 0 & 0 & 0 \\ \Delta t & 1 & 0 & 0 & 0 & 0 & 0 \\ \frac{\nu}{2}\Delta t^2 & \nu\Delta t & 1 & 0 & 0 & \mu\Delta t & 0 \\ 0 & 0 & 0 & 1 & -\dot{\varphi}\Delta t & 0 & 0 \\ 0 & 0 & 0 & \dot{\varphi}\Delta t & 1 & 0 & 0 \\ 0 & 0 & 0 & 0 & 0 & 1 & 0 \\ 0 & 0 & 0 & 0 & 0 & \lambda\Delta t & 1 \end{bmatrix}, \quad \begin{pmatrix} \delta\dot{a} \\ \delta\boldsymbol{\alpha} \end{pmatrix}_\mathsf{F} = \boldsymbol{\Phi}_{F,0}\begin{pmatrix} \delta\dot{a} \\ \delta\boldsymbol{\alpha} \end{pmatrix}_0 \tag{5}$$

$$\nu = -\tfrac{3}{2}n \qquad \dot{\varphi} = \tfrac{3}{2}n\gamma(5\cos^2 i - 1) \qquad \mu = -\tfrac{21}{2}n\gamma\sin 2i \qquad \lambda = 3n\gamma\sin^2 i$$

where γ is function of the J_2 coefficient, the orbit altitude, and an eccentricity factor.
At the guidance level the evolution $\mathbf{P}_0 \rightarrow \mathbf{P}_\mathsf{F}$ is given by:

$$\mathbf{P}_\mathsf{F} = \boldsymbol{\Phi}_{F,0}\mathbf{P}_0 + \boldsymbol{\Phi}_{F,1}a(\Delta\delta\boldsymbol{\alpha})_1 + \cdots + \boldsymbol{\Phi}_{F,m}a(\Delta\delta\boldsymbol{\alpha})_\mathsf{m} \tag{6}$$

Taking into account the structures of Eq. 3 and Eq. 5, the optimum problem of minimizing J_{plan} while satisfying the end conditions Eq. 6, consists in two disjointed subproblems in the subsets $(\boldsymbol{\Delta}\delta\dot{a}, \boldsymbol{\Delta}\delta a, \boldsymbol{\Delta}\delta\lambda, \boldsymbol{\Delta}\delta i_x, \boldsymbol{\Delta}\delta i_y)$ and $(\boldsymbol{\Delta}\delta e_x, \boldsymbol{\Delta}\delta e_y)$. They can be solved in the same

way by rearranging Eq. 6 as follows:

$$\left[\underbrace{\boldsymbol{\Phi}^{\delta*}_{\mathsf{F},1} \quad \cdots \quad \boldsymbol{\Phi}^{\delta*}_{\mathsf{F},m-1} \quad \boldsymbol{\Phi}^{\delta*}_{\mathsf{F},m}}_{\text{first column}} \cdots \underbrace{\boldsymbol{\Phi}^{\delta*}_{\mathsf{F},1} \quad \cdots \quad \boldsymbol{\Phi}^{\delta*}_{\mathsf{F},m-1} \quad \boldsymbol{\Phi}^{\delta*}_{\mathsf{F},m}}_{\text{last column}}\right] \begin{pmatrix} x_{1,1} \\ \vdots \\ x_{1,m} \\ \vdots \\ x_{p,1} \\ \vdots \\ x_{p,m} \end{pmatrix} = \mathbf{b}_0 \tag{7}$$

$$\mathbf{b}_0 = \mathbf{P}_{\mathsf{F}} - \boldsymbol{\Phi}_{\mathsf{F},0}\mathbf{P}_0$$

where the vectors $(\mathbf{x}_1, \cdots, \mathbf{x}_p)$ on turn assume the meaning of $(\boldsymbol{\Delta}\delta\dot{a}$,$a\boldsymbol{\Delta}\delta a$,$a\boldsymbol{\Delta}\delta\lambda$,$a\boldsymbol{\Delta}\delta i_x$, $a\boldsymbol{\Delta}\delta i_y)$ and $(a\boldsymbol{\Delta}\delta e_x, a\boldsymbol{\Delta}\delta e_y)$. As long as Eq. 4 is constant over a reconfiguration, the equations in $\boldsymbol{\Delta}\delta\dot{a}$ do not bring any information. Thus the effect of the differential drag is condensed in $\mathbf{b}_0$, that is in the total change of the δa and $\delta\lambda$ components, in agreement with [4]. The remaining equations constitute the two subproblems with $p = 4$ and $p = 2$ respectively. As a first step Eq. 6 is used to express the m-th ROE variations (i.e. $x_{j,m}$) as function of the first $m-1$ referred as $\tilde{\mathbf{x}}_j$. By substituting them back in Eq. 3, also the merit function depends only on these $m-1$ jumps. The necessary conditions for optimality are:

$$\frac{\partial J_{\mathsf{plan}}}{\partial \tilde{\mathbf{x}}_j} = \mathbf{0}^{\mathsf{T}}_{1\times m-1} \qquad j = 1, \cdots, p \tag{8}$$

Due to the forms of the merit function and of the variables' domain, these are also the sufficient conditions to identify the unique minimum of J_{plan}. Moreover the optimal solution reduces to solve a linear system in the problem's variables. This means that the particular choice of the parameterization allows solving the optimum problem for the dynamical system as a geometrical problem, whose solution is the most convenient succession of reachable points P_i in the ROE space.
The transition matrix of the $\delta a/\delta\lambda/\delta\mathbf{i}$ subproblem satisfies the following property:

$$\boldsymbol{\Phi}(t_j, t_i) \cdot \boldsymbol{\Phi}(t_i, t_k) = \boldsymbol{\Phi}(t_j, t_k) \tag{9}$$

thus the solution of Eq. 8 is given by:

$$\begin{aligned} \begin{pmatrix} \tilde{\mathbf{x}}_1 \\ \vdots \\ \tilde{\mathbf{x}}_4 \end{pmatrix}_{opt} &= \begin{bmatrix} \mathbf{I} + \eta\mathbf{A} + \nu^2\mathbf{C} & \nu\mathbf{D} & \nu\mu\mathbf{C} & \mathbf{O} \\ \nu\mathbf{D}^{\mathsf{T}} & \mathbf{I} + \mathbf{A} & \mu\mathbf{D}^{\mathsf{T}} & \mathbf{O} \\ \mu\nu\mathbf{C} & \mu\mathbf{D} & \mathbf{I} + \eta\mathbf{A} + \mu^2\mathbf{C} + \lambda^2\mathbf{C} & \lambda\mathbf{D} \\ \mathbf{O} & \mathbf{O} & \lambda\mathbf{D}^{\mathsf{T}} & \mathbf{I} + \mathbf{A} \end{bmatrix}^{-1} \mathbf{b}_0 \\ \mathbf{b}_0 &= \begin{pmatrix} b_{0,1}\tilde{\mathbf{a}} + \nu b^*_{0,2}\tilde{\mathbf{c}} \\ b^*_{0,2}\tilde{\mathbf{a}} \\ b_{0,3}\tilde{\mathbf{a}} + (\mu b^*_{0,2} + \lambda b^*_{0,4})\tilde{\mathbf{c}} \\ b^*_{0,4}\tilde{\mathbf{a}} \end{pmatrix}, \quad \begin{aligned} b^*_{0,2} &= b_{0,2} - \nu b_m b_{0,1} - \mu b_m b_{0,3} \\ b^*_{0,4} &= b_{0,4} - \lambda b_m b_{0,3} \end{aligned} \end{aligned} \tag{10}$$

The matrix quantities are $\mathbf{A} = \tilde{\mathbf{a}}\,\tilde{\mathbf{a}}^\mathsf{T}$, $\mathbf{C} = \tilde{\mathbf{c}}\,\tilde{\mathbf{c}}^\mathsf{T}$, $\mathbf{D} = \tilde{\mathbf{c}}\,\tilde{\mathbf{a}}^\mathsf{T}$, and the so far unmentioned notation is defined as:

$$\tilde{\mathbf{a}}_{m-1\times 1} = \begin{pmatrix} 1 \\ \vdots \\ 1 \end{pmatrix} \qquad \mathbf{b}_{m\times 1} = \begin{pmatrix} t_F - t_1 \\ \vdots \\ t_F - t_m \end{pmatrix} = \begin{pmatrix} \tilde{\mathbf{b}}_{m-1\times 1} \\ b_m \end{pmatrix} \qquad \tilde{\mathbf{c}} = \tilde{\mathbf{b}} - b_m\,\tilde{\mathbf{a}} \tag{11}$$

where $\tilde{\bullet}$ labels vectors of dimension $m-1$.
The time composition of state transition matrix of the relative eccentricity vector subproblem is instead:

$$\mathbf{\Phi}^{\delta\mathbf{e}}(t_j,t_i)\cdot\mathbf{\Phi}^{\delta\mathbf{e}}(t_i,t_k) = \mathbf{\Phi}^{\delta\mathbf{e}}(t_j,t_k) - \dot{\varphi}^2(t_j-t_i)(t_i-t_k)\cdot\mathbf{I}_{2\times 2} \doteq \widetilde{\mathbf{\Phi}}^{\delta\mathbf{e}}(t_j,t_k) \tag{12}$$

In order to lead back $\delta\mathbf{e}_0 \to \delta\mathbf{e}_\mathsf{F}$ to the form of Eq. 7, the following approximation is introduced:

$$\mathbf{\Phi}^{\delta\mathbf{e}}(t_h,t_j)\cdot\widetilde{\mathbf{\Phi}}^{\delta\mathbf{e}}(t_j,t_k) \approx \widetilde{\mathbf{\Phi}}^{\delta\mathbf{e}}(t_h,t_k) \tag{13}$$

coherently all the matrices that compare in Eq. 7, with exception of $\mathbf{\Phi}^{\delta\mathbf{e}}_{\mathsf{F},m}$, become of the type defined in Eq. 12. This approximation starts introducing some errors from the third maneuver window on. There are neglected terms of $\dot{\varphi}^2\Delta t^2$ with respect to the unit diagonal, and $\dot{\varphi}^3\Delta t^3$ in the extra-diagonal components.
By keeping $\tilde{\mathbf{a}}$, modifying $\mathbf{b} = \dot{\varphi}\mathbf{b}$, and introducing this further vectors:

$$\begin{aligned} &\tilde{\mathbf{d}}_{m-1\times 1} = \dot{\varphi}\begin{pmatrix} t_m - t_1 \\ \vdots \\ t_m - t_{m-1} \end{pmatrix} && \tilde{\mathbf{d}}_{m-1\times 1} = \dot{\varphi}\begin{pmatrix} t_{m-1} - t_1 \\ \vdots \\ t_{m-1} - t_{m-1} \end{pmatrix} \\ &\tilde{\mathbf{r}} = \tilde{\mathbf{a}} - b_m\tilde{\mathbf{d}} \ \text{ if } t_\mathsf{F} > t_m && \tilde{\mathbf{r}} = \tilde{\mathbf{a}} - \dot{\varphi}(t_m - t_{m-1})\tilde{\mathbf{d}} \ \text{ if } t_\mathsf{F} = t_m \end{aligned} \tag{14}$$

the solution of the optimum problem becomes:

$$\begin{pmatrix} \tilde{\mathbf{x}} \\ \tilde{\mathbf{y}} \end{pmatrix}_{opt} = \begin{bmatrix} \mathbf{I}+\mathbf{F}+\mathbf{G} & \mathbf{H}-\mathbf{H}^\mathsf{T} \\ \mathbf{H}^\mathsf{T}-\mathbf{H} & \mathbf{I}+\mathbf{F}+\mathbf{G} \end{bmatrix}^{-1} \begin{pmatrix} -\dfrac{b_{x0}+b_m b_{y0}}{1+b_m^2}\,\tilde{\mathbf{f}} + \dfrac{b_{y0}-b_m b_{x0}}{1+b_m^2}\,\tilde{\mathbf{g}} \\ -\dfrac{b_{x0}+b_m b_{y0}}{1+b_m^2}\,\tilde{\mathbf{g}} - \dfrac{b_{y0}-b_m b_{x0}}{1+b_m^2}\,\tilde{\mathbf{f}} \end{pmatrix} \tag{15}$$

where $\mathbf{F} = \tilde{\mathbf{f}}\,\tilde{\mathbf{f}}^\mathsf{T}$, $\mathbf{G} = \tilde{\mathbf{g}}\,\tilde{\mathbf{g}}^\mathsf{T}$, and $\mathbf{H} = \tilde{\mathbf{f}}\,\tilde{\mathbf{g}}^\mathsf{T}$ with:

$$\tilde{\mathbf{f}} = -\frac{1}{1+b_m^2}(\tilde{\mathbf{r}} + b_m\tilde{\mathbf{b}}) \qquad \tilde{\mathbf{g}} = \frac{1}{1+b_m^2}(\tilde{\mathbf{b}} - b_m\tilde{\mathbf{r}}) \tag{16}$$

To conclude this section, the intermediate relative configurations output by the planning problem are computed from Eq. 6, once obtained the optimal variations of ROE from Eqs. 10 and 15.
It is emphasized that, due to the structure of the state transition matrix, one could solve this planning problem via a *geometrical* method which stepwise covers the aimed total variation of

ROE through corrections proportional to the covered time portion. The result obtained would be the same as long as J_{plan} describes the delta-v in terms of the size of the ROE total jump. Nevertheless the proposed method offers a rigorous approach that shows that such solution guarantees the minimum delta-v, being as well suitable for an automated implementation. Moreover this approach provides a working frame ready to support possible improvements, as for example, introducing constraints directly at the planning level, as penalties function of the variations of ROE $(\Delta\delta\boldsymbol{\alpha})_i$.

4. The Local Control Problem

Within the architecture described so far, the local control problem solves a fixed-time, fixed-end-condition problem. Type and number of impulses are respectively fixed by minimum delta-v considerations and by the existence of an analytical solution. At each local problem the maneuvers shall accomplish the following variation of ROE over the time span $[t_{0i}, t_i]$:

$$a\Delta\delta\tilde{\boldsymbol{\alpha}} = a\delta\boldsymbol{\alpha}_i - \boldsymbol{\Phi}_{i,0i} a\delta\boldsymbol{\alpha}_{0,i} \tag{17}$$

The out-of-plane correction is decoupled from the in-plane one. It is obtained by a single maneuver placed either at u_{oop} or at $u_{\text{oop}} + \pi$ according to:

$$u_{\text{oop}} = \arctan\left(\frac{\Delta\delta\tilde{i}_y}{\Delta\delta\tilde{i}_x}\right) \qquad \text{with} \qquad |\delta v_n| = na\left\|\Delta\delta\tilde{\mathbf{i}}\right\| \tag{18}$$

where the sign of δv_n is chosen so that the last two end-conditions of Eq. 17 are satisfied.
The relations between an instantaneous velocity increment in the Hill's orbital frame and the consequent change of ROE are obtained from the inversion of the adopted linear model [4, p.41]. It can be seen that a minimum of two maneuvers are required to meet a whatever in-plane end-conditions' set. Thus, by assuming as problem variables the magnitudes and locations of such maneuvers, the local control in-plane subproblem to satisfy Eq. 17 is under-determined. As long as we are interested in solutions that minimize the delta-v consumption, the size of the solution space can be reduced by employing only tangential burns, since they allow consuming less delta-v while affecting all the in-plane ROE terms, either instantaneously or within a certain timespan. On one hand, if only two tangential burns were used, it would not be always possible to satisfy all the possible end-conditions' sets. On the other hand, by employing three tangential impulses an analytical solution of Eq. 17 always exists, upon the condition of performing such maneuvers at integer half orbital period multiples of a fixed mean argument of latitude. In particular the satisfaction of Eq. 17 implies that such required location is exactly the phase angle of the aimed variation of the relative eccentricity vector:

$$\bar{u} = \text{mod}\left(\arctan\left(\frac{\Delta\delta\tilde{e}_y}{\Delta\delta\tilde{e}_x}\right), \pi\right) \qquad u_{\text{ip}j} = \bar{u} + k_j\pi, \qquad j = 1...3 \qquad k_1 < k_2 < k_3 \tag{19}$$

In the limited time horizon of each control window there exist a finite number of possible solutions, depending on the values assumed by k_j. The correspondent delta-v quantities are computed according to Tables 1 and 2. There the following notation is adopted: $a\Delta\delta\tilde{\boldsymbol{\alpha}}_{\text{ip}} = (A, L, E, F)^{\mathsf{T}}$, $q = u_i - u_{\text{ip1}}$, $p = u_i - u_{\text{ip2}}$, and $l = u_i - u_{\text{ip3}}$; where u_i represents the end-time

Table 1. Feasible solution families depending on the aimed end-conditions.

Aimed end-conditions			Choice of k_j	$\delta\tilde{v} = \dfrac{bA + gB}{4b}$	
	B	b	Signs	$+--,--+,-+-$	$+-+,++-,-++$
$\bar{u} \in [0, \pi/2)$	E	$\cos\bar{u}$	sign($\cos u_{\text{ip}j}$)	$g = 1$	$g = -1$
$\bar{u} = \pi/2$	F	$\sin\bar{u}$	sign($\sin u_{\text{ip}j}$)		
$\bar{u} \in (\pi/2, \pi)$	E	$\lvert\cos\bar{u}\rvert$	sign($\cos u_{\text{ip}j}$)	$g = -1$	$g = 1$

Table 2. All possible delta-v values for the triple-tangential fixed $\bar{u}$ solution scheme, once derived *Signs* and *g* from Table 1.

Signs	$\delta\tilde{v}$	D	Remaining delta-v expressions
$+--$ $-++$	δv_1	$12b(p-l)$	$\delta v_2 = -\left(4b\,L + 3g(q-l)\,B + 3b(q+l)\,A\right)/D$ $\delta v_3 = +\left(4b\,L + 3g(q-p)\,B + 3b(q+p)\,A\right)/D$
$--+$ $++-$	δv_3	$12b(q-p)$	$\delta v_1 = -\left(4b\,L - 3g(p-l)\,B + 3b(p+l)\,A\right)/D$ $\delta v_2 = +\left(4b\,L - 3g(q-l)\,B + 3b(q+l)\,A\right)/D$
$-+-$ $+-+$	δv_2	$12b(q-l)$	$\delta v_1 = -\left(4b\,L + 3g(p-l)\,B + 3b(p+l)\,A\right)/D$ $\delta v_3 = +\left(4b\,L - 3g(q-p)\,B + 3b(q+p)\,A\right)/D$

limit t_i of the control window. The criterion to select one solution among all these possible ones is explained in section 7.

5. Safety Concept

Passive safety is based on keeping a certain minimum separation between the satellites in the radial–cross-track plane. Thus it is related to the δe and δi magnitudes and to the angular separation between the relative eccentricity and inclination vectors $\phi = \varphi - \theta$ [4, p.29] and [9]. Let us focus on the behavior of the ROE in the $\delta\mathbf{e}$ and $\delta\mathbf{i}$ planes determined by the functioning of the local control and planning units. At the local level, the single out-of-plane maneuver moves the relative inclination vector directly from its starting to its final place. In the mean time the relative eccentricity vector covers the aimed jump in three steps, displaced along the direction of $\Delta\delta\mathbf{e}_i$ vector. If an optimal solution is available, all the locations are contained in the $\Delta\delta\mathbf{e}_i$ segment. On the contrary, if the change in the shape of the orbit is not the dominant effect of the *i*-th reconfiguration or if the control window is not long enough to support an optimal scheme, at least an intermediate eccentricity vector location resides outside the segment $\Delta\delta\mathbf{e}_i$. However by selecting the minimum delta-v option the length of the realized total relative eccentricity vector variation is the minimum possible obtainable, thus points would be not spread too far from each other. At the planning level, Eq. 3 entails selecting intermediate $\mathbf{P}_i$ so that the total length to reach $\mathbf{P}_\text{F}$ is minimized. Thus the obtained configurations lay as most as possible aligned to the $\mathbf{P}_\text{F}$-$\mathbf{P}_0$ line. Therefore their projections on the unit-circle in the

$\delta\mathbf{e}/\delta\mathbf{i}$ plane condense in a limited portion of the space.
Taking into account all these considerations whenever a safe $\mathbf{P}_\mathsf{F}$ (adequate ϕ_F) is reached from a $\mathbf{P}_0$ with similar characteristics (i.e. $\phi_0 \approx \phi_\mathsf{F}$) than the reconfiguration is passively safe during the whole duration of the reconfiguration. On the other hand, in the specific scenario of a far-range rendezvous to a non cooperative target starting from an unsafe ϕ_0, a double stage strategy can be exploited being $\mathbf{P}_\mathsf{F}$ a design parameter of the reconfiguration. First ϕ_0 can be corrected when the along-track separation is considerable, by commanding a safe temporary final configuration. Subsequently the approach can safely start towards an aimed $\mathbf{P}_\mathsf{F}$ closer to the target.

6. Time Constraints Handling

According to the planner interfaces shown in Fig. 1, the user provides a list of times limiting periods in which it is not possible to schedule maneuvers due to possible requirements of the space segment (see section 2). Moreover, when in *maximum observability* mode, the user can define time barriers before which some maneuvers shall occur (see section 2.1). These informations are handled by the scheduling functionality to determine the initial and final times of each interval in which it is allowed performing maneuvers. In the case that any free time interval among two forbidden regions is shorter than two orbital periods, such portion of the schedule is merged to the forbidden part. That is motivated from how the local control function operates: the fastest in-plane reconfiguration exploits a train of three half-orbital-period spaced impulses; the out-of-plane maneuver has to be distant enough from each of them to fulfill the *maneuvers' spacing* time constraints. Moreover a forbidden time region is also placed at the re-plan time t_0 to prevent scheduling early maneuvers that would violate the *time to first maneuver* constraint.
If in *maximum observability* mode, the obtained list of end-times of the control windows is provided to the planning unit that outputs the correspondent intermediate configurations P_i to be established. Consequently the only remaining action to assess the feasibility of the whole reconfiguration plan would be to schedule out-of-plane maneuvers in accordance to the maneuvers' spacing time constraints, (see section 8).

7. In-plane Maneuvers' Placement

The placement of the in-plane maneuvers finalizes the local control problem activity as its objective is to select one maneuver scheme among the multiple available possibilities. As explained in section 4, in fact, when an in-plane reconfiguration is performed through three tangential impulses multiple solutions are feasible, depending on the effective spacing between the burns (see Tables 1 and 2). The logic to perform such choice is presented in Fig. 2. According to it, all schemes of the limited set of feasible solutions are sequentially processed; it is selected the option that successfully terminates that logical tree. In *minimum delta-v* mode a feasibility check (gray dashed box) has to be performed prior to the remaining evaluations. Only solutions whose maneuvers are located in constraints-free regions can proceed. Further, minimum delta-v options are preferred. In case of multiple equal delta-v options it is preferred the solution that is characterized by a wider spacing between two of the three burns. This is motivated by the preference to leave more freedom to the remaining actions of the planner.

Thus, byproduct of the unit is the end-time of the sub control window dedicated to the out-of-plane burn $t_{i,\text{oop}}$. It is emphasized that, a solution is always determined due to the fact that the scheduling does not allow having maneuvering windows shorter than two orbital periods.

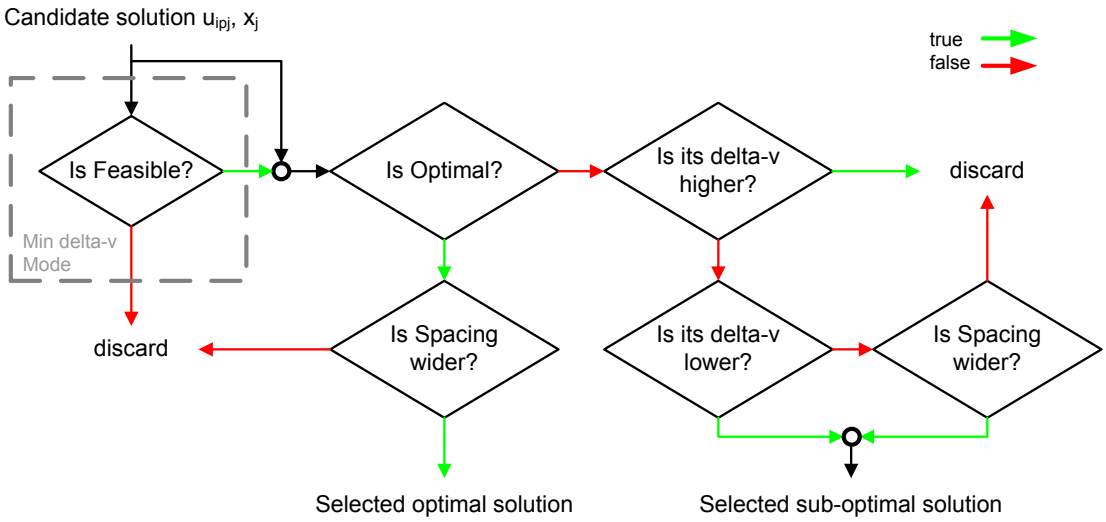

Figure 2. Logic of the in-plane maneuvers' scheme selection.

8. Out-of-plane Maneuvers' Placement

This last part schedules the out-of-plane maneuver of each control window during the orbital period time that ends at $t_{i,\text{oop}}$, according to Eq. 18. Only in case of tight maneuver window and u_{oop} closer to $\bar{u}$ than the maneuvers' spacing time constraint, the out-of-plane burn is merged with an in-plane one. In this situation a normal delta-v component is scheduled at the time of the in-plane maneuver with most similar magnitude to the required out-of-plane one, to reduce the effects of the maneuver execution errors.

9. Example of a Rendezvous

This section is intended to show the functioning of the maneuver planner. To this end, a representative test case of a rendezvous has been defined. According to it a chaser satellite has to approach a target moving from an initial separation of circa 10 km to a final one of 3 km. The details of the initial and final conditions in ROE are presented in Table 3: $\mathbf{P}_\text{F}$ is a bounded relative orbit with anti/parallel $\delta\mathbf{e}$ and $\delta\mathbf{i}$. At the beginning the relative orbit has a bigger size (δe and δi magnitudes) than the aimed one. Moreover there are some errors in the x components of both relative eccentricity and inclination vectors. The generation of the plan occurs at a time t_0 in which the mean argument of latitude of the chaser is 0 degrees. At that time the chaser satellite is on a circular orbit 500 km high with 98 degrees of inclination. The approach has to be covered in 18 orbital periods, that is approximately in 28 hours. At the height of the chaser spacecraft the atmospheric density is equal to 1 g/km^3 for mean solar flux conditions (Harris Priester model [10]) and the relative velocity is circa 7.6 km/s. In the example treated it is assumed that the target has a ballistic coefficient B of 0.01 m^2/kg and the differential ballistic

Table 3. Example's scenario and intermediate configurations.

Input	Intermediate	$a\delta\boldsymbol{\alpha}$ [m]					
$\mathbf{P}_0$		5	10000	-50	-250	-30	200
	$\mathbf{P}_1$	54.6	9814.2	-34.1	-199.3	-22.1	166.7
	$\mathbf{P}_2$	48.1	5714.2	-19.0	-149.0	-11.9	132.9
$\mathbf{P}_\mathsf{F}$		0	3000	0	-100	0	100

coefficient $\Delta B/B$ is 2%.
Let us consider that for any reason the user commands to the spacecraft to avoid maneuvering respectively from 5 to 7 and from 12 to 14 orbits after the plan generation time. Moreover, in view of the *maximum observability* mode, he commands that a reconfiguration shall occur within the first 4 orbital periods starting from t_0. From Fig. 3, where all time constrained regions are shadowed in gray, one can note that this last requirement is merged with the first forbidden time interval and that t_0 occurs at orbit 1. In the example treated both time to first maneuver and time spacing between maneuvers are set equal to 10 minutes.
When planning in *minimum delta-v* mode, the plan reported in the left view of Fig. 3 is generated. In particular in this case the reconfiguration happens in one step over the complete time horizon; the most relevant change is in $\Delta\delta\mathbf{e}$ and the optimality criterion based on the lower bound of the delta-v is applicable. The schemes of Tables 1 and 2 generate 216 feasible optima solutions subsequently pruned by the logic of section 7. This constitutes a generalization of the approach of Ref. [6] to cope with the presence of time constraints. The total delta-v is of circa 0.20 m/s.
The right view of Fig. 3 shows the maneuvers' plan generated in the *maximum observability* mode. There the intermediate configurations $\mathbf{P}_1$ and $\mathbf{P}_2$ of Table 3 are to be achieved respectively within 4 and 12 orbital periods after t_0. According to the required variations of ROE, for each of these three reconfigurations $\Delta\delta\mathbf{e}$ is not the dominant change to be achieved. Hence the local control can accomplish only suboptimal solutions, among them the best ones have been selected according to sections 7 and 8. Tangential (green) and normal (blue) maneuvers are automatically scheduled, in agreement with maneuvering spacing constraints. The total realized delta-v is of circa 0.217 m/s; as expected slightly higher than in the previous case.

Taking into account the magnitudes and the configurations of the $\delta\mathbf{e}$ and $\delta\mathbf{i}$ vectors both rendezvous options are passively safe. This is shown by both top views of Fig. 3 where are reported the relative eccentricity (marked with squares) and the relative inclination (marked with circles) unit vectors achieved after each maneuver. The later the maneuver the lighter the color of the marker.
Figure 4 focuses on the maneuvers' plan obtained in the *maximum observability* mode, in order to visualize what is the resultant behavior of the relative motion. To this end the ROE are propagated over time making use of the model discussed in section 3, since we are focusing on a qualitative analysis. Maneuvers are introduced as instantaneous ROE discontinuities at the proper mean arguments of latitude. The left view of Fig. 4 reports the intermediate $\delta\mathbf{e}$ and $\delta\mathbf{i}$ locations which, as expected, distribute around the directions of their respective total

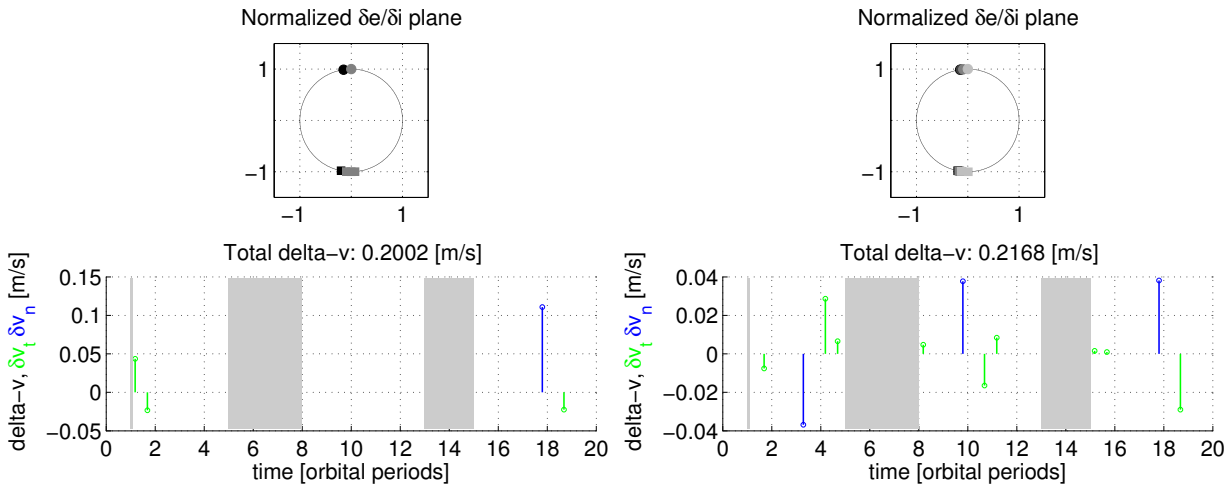

Figure 3. Maneuvers' plan in both the operative modes for the rendezvous of Table 3.

aimed variations. The right view shows instead how the approach is obtained by establishing a certain relative semi-major axis at the beginning of the plan. Such drift is canceled in proximity of the aimed final separation. This behavior is determined by the attempt to employ the minimum possible delta-v; hence exploiting at maximum the available time horizon. In realistic applications this aspect shall be mitigated with a proper strategy of setting $\mathbf{P}_F$, as the chain of navigation and control errors can lead to an overshooting in the along-track direction.

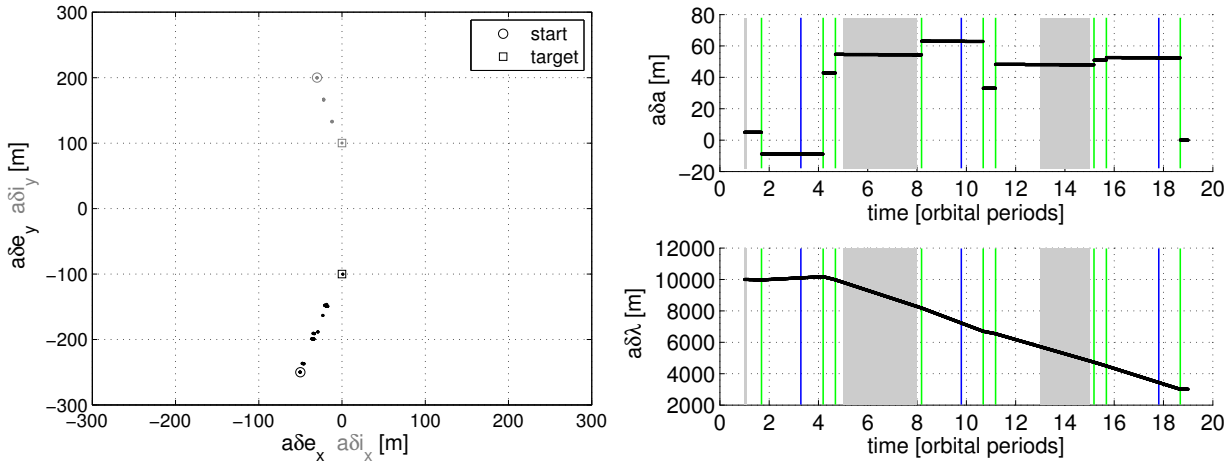

Figure 4. Rendezvous propagation in the ROE space.

10. Conclusions

This work addressed the design of a maneuvers' planner for formation flying reconfiguration. Its development was motivated by the design of the Autonomous Vision Approach Navigation and Target Identification (AVANTI) experiment to be conducted in the frame of the DLR FIREBIRD mission.
Simplicity and determinism constituted driver features in the development of the planner. This

turned out into the exploitation of the geometrical meaning of the relative orbital elements and of the existence of analytical solutions for accomplishing stepwise reconfigurations in a delta-v minimum manner. Despite this, the planner is able to meet important operational requirements like passive safety during a rendezvous. Moreover it offers the capability to introduce time constraints that prevent executing maneuvers in certain portions of the schedule.

11. References

[1] Bodin, P., Noteborn, R., Larsson, R., Karlsson, Th., D'Amico, S., Ardaens, J.-S., Delpech, M., and Berges, J.-C., "Prisma Formation Flying Demonstrator: Overview and Conclusions from the Nominal Mission," AAS 12-072, 35th Annual AAS Guidance and Control Conference, 3-8 Feb. 2012, Breckenridge, Colorado (2012).

[2] D'Amico, S., Ardaens, J.-S., and Larsson, R., "Spaceborne Autonomous Formation-Flying Experiment on the PRISMA Mission, " Journal of Guidance, Control, and Dynamics, Vol. 35, No.3, 2012, pp. 834-850.

[3] Ardaens, J.-S., D'Amico, S., and Fischer, D., "Early Flight Results from the TanDEM-X Autonomous Formation Flying System, " 4th International Conference on Spacecraft Formation Flying Missions & Technologies (SFFMT), 18-20 May 2011, St-Hubert, Quebec (2011).

[4] D'Amico, S., "Autonomous Formation Flying in Low Earth Orbit," Ph.D. Thesis, Technical University of Delft, 2010.

[5] D'Amico, S., Ardaens, J.-S., Gaias, G., Benninghoff, H., Schlepp, B., and Jørgensen, J.L., "Non- Cooperative Rendezvous using Angles-only Optical Navigation: System Design and Flight Results," accepted for publication in Journal of Guidance, Control, and Dynamics, 2013.

[6] Eckstein, M.C., "Generalized Maneuver Planning for Station Keeping, Station Acquisition, Longitude Transfer and Reorbiting of Geostationary Satellites," Technical Note, GSOC TN 92-6, Deutsches Zentrum für Luft- und Raumfahrt, November 1992.

[7] Ichimura, Y., and Ichikawa, A., "Optimal impulsive relative orbit transfer along a circular orbit," Journal of Guidance, Control, and Dynamics, Vol. 31, No.4, 2008, pp. 1014-1027.

[8] Gaias, G., D'Amico, S., and Ardaens, J.-S., "Angles-only Navigation to a Non-Cooperative Satellite using Relative Orbital Elements," AIAA/AAS Astrodynamics Specialists Conference, Minneapolis, MN, 13-16 August 2012.

[9] D'Amico, S., and Montenbruck, O., "Proximity Operations of Formation Flying Spacecraft using an Eccentricity/ Inclination Vector Separation," AIAA Journal of Guidance, Control and Dynamics, Vol. 29, No. 3, May-June 2006, pp. 554-563.

[10] Montenbruck, O., and Gill, E., "Satellite Orbits-Models, Methods, and Applications," Springer-Verlag, Heidelberg, Germany, 2001a.